Available online at www.sciencedirect.com
ScienceDirect
Journal of Organometallic Chemistry 692 (2007) 248–256
Journal of Organometallic Chemistry
www.elsevier.com/locate/jorganchem

Synthesis and molecular structures of S-2-FcNHCOC$_6$H$_4$SH and [M^{III}(OEP)(S-2-FcNHCOC$_6$H$_4$)] (Fc = ferrocenyl, M = Fe, Ga): Electrochemical contributions of intramolecular SH···O=C and NH···S hydrogen bonds

Taka-aki Okamura *, Taku Iwamura, Hitoshi Yamamoto, Norikazu Ueyama *

Department of Macromolecular Science, Graduate School of Science, Osaka University, Toyonaka, Osaka 560-0043, Japan

Received 28 February 2006; accepted 26 May 2006
Available online 30 August 2006

Abstract

A novel redox-active thiolate ligand having a ferrocene moiety, S-2-FcNHCOC$_6$H$_4$SH (**1a**), and its porphyrin-thiolate compounds, [M^{III}(OEP)(S-2-FcNHCOC$_6$H$_4$)] (M = Fe (**2a**), Ga (**3a**)) were synthesized and characterized by X-ray analysis, spectroscopic and electrochemical measurements. The corresponding 4-substituted derivatives (**1b**–**3b**) were also synthesized to estimate the contribution of substituent effects. The formation of intramolecular SH···O=C or NH···S hydrogen bonds in solution was established by ^{1}H NMR and IR spectra. The cooperative effects of the hydrogen bonds and π-conjugation were found on redox potentials of Fc and iron-porphyrin moieties.

Keywords: Ferrocene; Porphyrin; Hydrogen bond; Thiolate; Redox potential

1. Introduction

Ferrocene is the one of the most stable redox-active molecules and has been used for various applications including receptors or electrochemical sensing of small molecules [1–6]. In the recognition, intermolecular hydrogen bonds are formed resulting negative shift of the redox potential of metal center [2–6].

On the other hand, intramolecular NH···S hydrogen bond positively shifts the redox potential of various metal thiolates [7–13]. Especially, electron-withdrawing group, that is CF_3, strengthens the hydrogen bond which results in a large positive shift [3,7].

In this paper, we design a redox-active thiolate ligand and detect directly the electron flow or electrochemical coupling between ferrocene and (porphinato)iron(III) moieties through the hydrogen bonds.

2. Results

2.1. Molecular design and synthesis

Incorporation of *N*-alkylcarbamoyl group to benzenethiol presents us two types of hydrogen bonds, SH···O=C and NH···S. In thiol (**1a**), the carbonyl group forms SH···O=C hydrogen bond as shown in Scheme 1. When SH group of **1a** is deprotonated, the amide plane is flipped around the phenyl–carbonyl bond and NH···S hydrogen bond can form as shown for **2a** and **3a** in Scheme 1. To estimate induction effects, 4-substituted derivatives **1b**–**3b** were synthesized. Obviously, these compounds cannot form any intramolecular hydrogen bond.

* Corresponding authors. Tel.: +81 6 6850 5451; fax: +81 6 6850 5474.
E-mail addresses: tokamura@chem.sci.osaka-u.ac.jp (T. Okamura), ueyama@chem.sci.osaka-u.ac.jp (N. Ueyama).

0022-328X/$ - see front matter © 2006 Elsevier B.V. All rights reserved.
doi:10.1016/j.jorganchem.2006.08.067

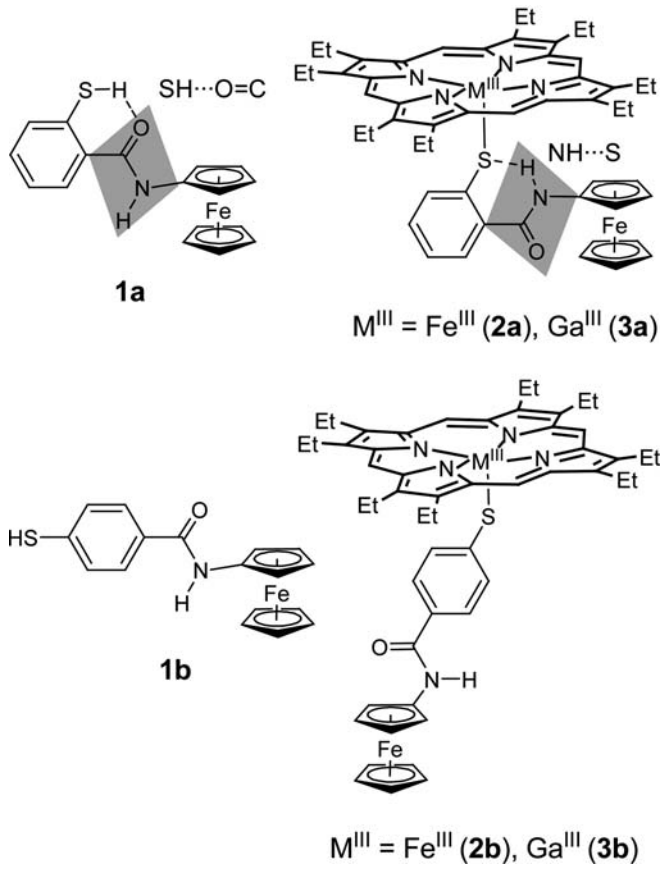

Scheme 1.

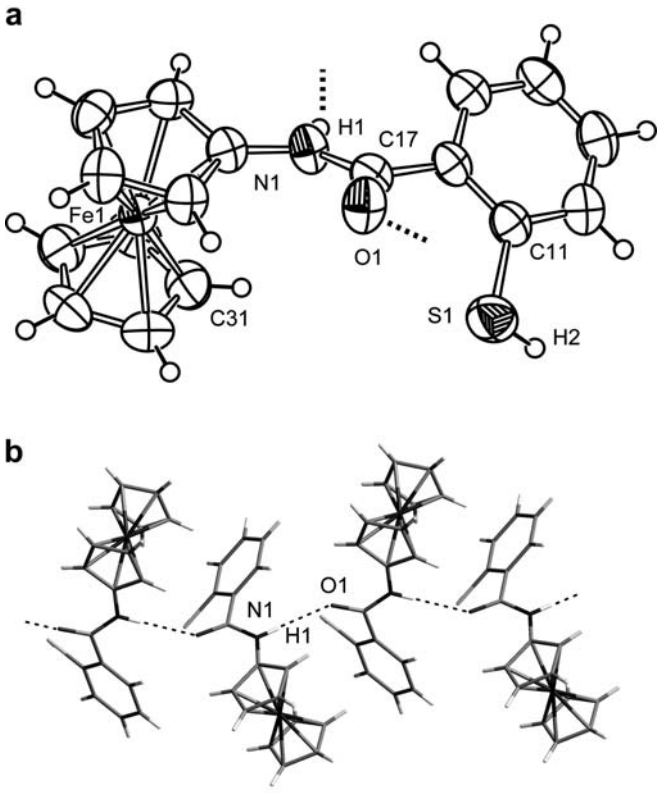

Fig. 1. (a) Molecular structure of 2-FcNHCOC$_6$H$_4$SH (**1a**) and (b) intermolecular NH ·· O=C hydrogen bond chain of **1a** in the crystal.

2.2. Molecular structures of 2-FcNHCOC$_6$H$_4$SH (*1a*) and [Ga^{III}(OEP)(S-2-FcNHCOC$_6$H$_4$)] (*3a*)

The molecular structure of **1a** is shown in Fig. 1. The thiol, **1a**, forms infinite intermolecular NH···O=C hydrogen bond chains in the crystal. The SH group does not form any significant hydrogen bond with an electronegative atom, i.e., O or S. The SH group is directed to the neighboring Cp (cyclopentadienyl) ring with a short contact (H2–C31 = 3.27(4)), which suggests the presence of an intermolecular SH···π interaction. The NH···O=C hydrogen bond is more effective than SH···O=C hydrogen bond to stabilize the packing energy.

For **3a**, two independent molecules were found in the unit cell. Two molecules do not show significant difference each other. One of them is shown in Fig. 2. The amide NH is directed to the thiolate S and forms intramolecular NH···S hydrogen bond with short N···S contact (ca. 3 Å). The selected bond lengths and angles are summarized in Table 1 comparing with some analogous. Two structures of (porphinato)gallium(III) thiolate complexes have been known [14]. Previously, we reported a significant contribution of intramolecular NH···S hydrogen bond to the elongation of Ga–S bond. The Ga–S bond distances of the molecules **3a** are 2.320(12) Å and 2.318(2) Å which are longer than that of [Ga^{III}(OEP)(SPh)] (2.274 Å) by

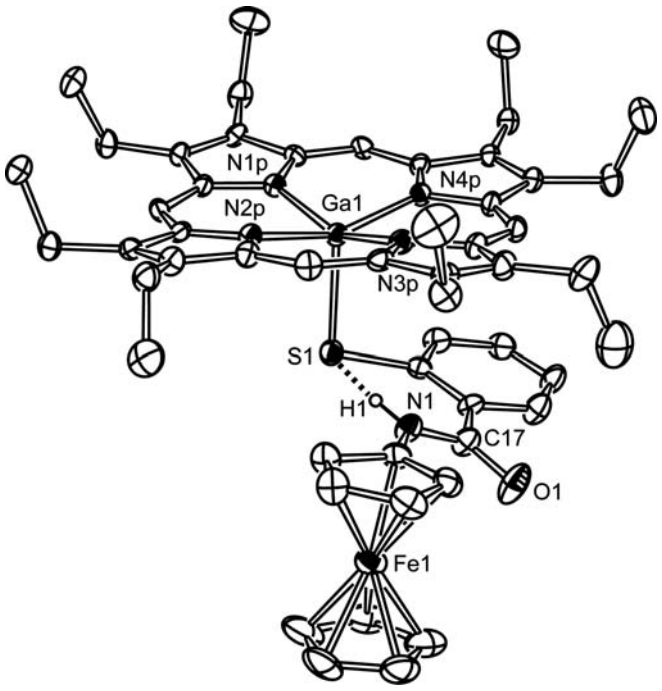

Fig. 2. Molecular structure of [Ga^{III}(OEP)(S-2-FcNHCOC$_6$H$_4$)] (**3a**). Two independent molecules are present in the unit cell. Two molecules do not show significant difference each other and one of them is shown here. The thermal ellipsoids are drawn at the 25% probability level.

Table 1
Selected bond distances (Å) and angles (°) of [Ga^{III}(OEP)(S-2-RC_6H_4)]

	R			
	FcNHCO (**3a**)		H	CF_3CONH[a]
Ga1–S1	2.320(2)	2.318(2)	2.274(2)	2.315(3)
Difference	+0.046	+0.044	0	+0.041
Ga1–N1p	2.044(5)	2.049(5)	2.043(6)	2.054(9)
Ga1–N2p	2.055(4)	2.028(4)	2.054(5)	2.022(6)
Ga1–N3p	2.039(5)	2.046(5)	2.038(6)	2.03(1)
Ga1–N4p	2.049(3)	2.057(4)	2.044(6)	2.005(7)
Mean	2.047	2.045	2.045	2.04
Ga1–N_4	0.412(3)	0.418(3)	0.457	0.3856
S1–C11	1.779(6)	1.791(6)	1.761(9)	1.753(9)
Ga1–S1–C11	101.9(2)	103.0(2)	103.5(3)	104.1(4)
Ga1–S1–C11–C12	−102.4(6)	95.6(6)	93.1(9)	−103.0(9)
N1···S1	3.075(5)	3.078(6)	–	2.92(1)
(N1)H···S1	2.318	2.313	–	2.390

[a] The data have been reported [14].

0.046 Å and 0.044 Å, respectively. These results strongly suggest the presence of interactions between the amide NH and the thiolato S.

2.3. Detection of hydrogen bonds

The stretching bands of amide and thiol groups are summarized in Tables 2 and 3. The formation of intra- or intermolecular hydrogen bonds were established by the significant lower-wavenumber shift. In the solid state, the thiol, 2-FcNHCOC_6H_4SH (**1a**), shows ν(NH), ν(C=O), and ν(SH) bands at 3301, 1637, and 2575 cm^{-1}, respectively. The lower-shifted bands indicate the presence of intermolecular NH···O=C hydrogen bonds in the comparison with free ν(NH) (3439 cm^{-1}) and ν(C=O) (1673 cm^{-1}) of $FcNHCOCH_3$. These results are consistent with the crystal structure. On the other hand, **1a** forms an intramolecular SH···O=C hydrogen bond in chloroform-d_1. ν(NH) (1665 cm^{-1}) and ν(SH) (2564 cm^{-1}) were observed at lower wavenumbers. Such a hydrogen-bonded SH was also detected as a minor peak in the solid state (Table 2). When **1a** was deprotonated to (NEt_4)[S-2-FcNHCOC_6H_4] (**4a**), unusually low-wavenumber-shifted ν(NH) was found at 3044 cm^{-1}, while 4-substituted derivative (**4b**) shows no significant shift [15]. These results agree with the proposed molecular structures of **1a** and **2a** illustrated in Scheme 1. This proposal is supported by ^{1}H NMR spectra discussed below.

Table 3
IR spectral data in CH_2Cl_2 for various compounds

Compounds	ν(NH)/cm^{-1}	ν(CO)/cm^{-1}	ν(SH)/cm^{-1}
2-FcNHCOC_6H_4SH (**1a**)	3424	1667	2547
4FcNHCOC_6H_4SH (**1b**)	3440	1672	2583
[Fe^{III}(OEP)(S-2-FcNHCOC_6H_4)] (**2a**)	3195	1651	–
[Fe^{III}(OEP)(S-4-FcNHCOC_6H_4)] (**2b**)	3441	1671	–
[Ga^{III}OEP](S-2-FcNHCOC_6H_4)] (**3a**)	3184	1651	–
[Ga^{III}(OEP)(S-4-FcHCOC_6H_4)] (**3b**)	3445	1670	–
(NEt_4)[S-2-FcNHCOC_6H_4] (**4a**)	3044	1623	–
(NEt_4)[S-4-FcNHCOC_6H_4] (**4b**)	3450	1645	–
$FcNHCOC_6H_5$	3439	1673	–

The ^{1}H NMR signals of amide NH and SH protons for these compounds are listed in Table 2. The down-field-shifted signals indicate the formation of intramolecular hydrogen bonds. Especially, **4a** indicates extraordinary large value (14.21 ppm) for an amide proton. The other NH peaks were found in usual region. The substituent effect of thiolate anion is limited within a relatively small shift (1.1 ppm for **4b**). Acylaminoferrocenes form relatively strong hydrogen bonds due to the acidic NH proton induced by delocalization of electron on NH to Cp ring as described in the previous papers [16–18].

In the porphinato compounds, [M(OEP)(S-2-FcNHCOC_6H_4)] (M = Fe^{III}(**2a**) and Ga^{III} (**3a**)), NH···S hydrogen bonds were detected by IR absorption in dichloromethane (Table 3). The NH stretching band of **3a** was found at a lower wavenumber (3184 cm^{-1}) than that of **2a** (3195 cm^{-1}). Such a stronger NH···S has been found previously, which is caused by a more ionic Ga–S bond than Fe–S [14]. The ionic bond prevents the decrease of electron density on S by π-donation from the thiolato ligand to the metal ion and the electron-rich sulfur has considerably strong ability of hydrogen bond formation.

2.4. ^{1}H NMR of porphinato compounds

The porphinato compounds have been known for the large dipolar shift caused by the expanded ring current. [Ga(OEP)(S-2-FcNHCOC_6H_4)] (**3a**) exhibits proton reso-

Table 2
IR and ^{1}H NMR spectral data of thiols and thiolates

Compounds		IR/cm^{-1}			^{1}HNMR δ/ppm	
		ν(NH)	ν(CO)	ν(SH)	NH	SH
2-FcNHCOC_6H_4SH (**1a**)	In $CDCl_3$	3432	1665	2564	7.10	4.66
	Solid	3301	1637, (1627)[a]	2575 (2560)	–	–
4-FcNHCOC_6H_4SH (**1b**)	In $CDCl_3$	3447	1672	2587	7.10	3.59
	Solid	3309	1633	2573, 2563	–	–
(NEt_4)[S-2-FcNHCOC_6H_4] (**4a**)	In $CDCl_3$	3044	1623	–	14.21	–
(NEt_4)[S-4-FcNHCOC_6H_4] (**4b**)	In $CDCl_3$	3450	1645	–	8.26	–
$FcNHCOC_6H_5$	In $CDCl_3$	3446	1673	–	7.16	–

[a] The minor peaks (30% intensity) are shown in the parentheses.

nances of ethyl groups at 3.91, 4.02 (CH_2), and 1.87(CH_3) ppm in benzene-d_6. These values were found in a reasonable region for 5-coordinated porphinato(thiolato) compounds reported previously [14]. Furthermore, paramagnetic iron(III) center effectively shifts the proton signal by electron spin–nuclear spin interactions through bonds and/or space. The observed chemical shifts of **2a** and **2b** in benzene-d_6 are shown in Table 4.

In the case of paramagnetic compounds, the signal signs of the aromatic protons are explained by the alternative rule of electron spins in a conjugated system [7,8]. The N^1H signal of **2a** was found as a very broad peak that was confirmed at −98.4 ppm by ^2H NMR of NH-deuterated **2a** (Fig. 3). When an amide group was introduced to 4-position, [Fe(OEP)(S-4-FcNHCOC$_6$H$_4$)] (**2b**), the NH peak was found at 33.7 ppm. The unusual upper-field shift of **2a** strongly suggests the presence of a direct interaction through NH···S hydrogen bond. If the NH···S bond is not present, the signal must be found at a lower field as found for **2b**. Moreover, the shift (ca. −100 ppm) is larger than the reported values (ca. −50 ppm) for hydrogen-bonded compounds, e.g., [Fe(OEP)(S-2-CF$_3$CONHC$_6$H$_4$)] [7]. In the case of **2b**, Fe^{III}-thiolate bond is broken to form Fe^{II} and disulfide by redox equilibrium [19]. The presence (20%) of [Fe^{II}(OEP)] was detected by ^1H NMR. Such a behavior has been known for usual iron(III) (thiolato)porphinato complexes.

2.5. Electrochemical studies

The compounds **1a**–**3b** show reversible Fe^{III}/Fe^{II} redox couple due to ferrocene moiety in dichloromethane. The iron(III) porphinato derivatives, **2a** and **2b**, show additional quasi-reversible one. The $E_{1/2}$ values (vs. Ag/Ag^+) are summarized in Table 5. These values were within an error of about 2 mV for several measurements. Non-substituted ferrocene indicated the redox potential at 191 mV under the same condition. The 2-substituted derivatives exhibit more positive potential than the 4-substituted ones. The trend, thiol > Fe-porphyrin > Ga-porphyrin, was found for these derivatives, which is consistent with the covalency of S–X where X is proton or metal ion, suggesting that it reflects the electronic negativity on the sulfur atom.

At the metalloporphyrin site, **2a** shows a remarkable positive shift (by 120 mV) than **2b**. According to the reported conditions, the redox potentials were observed at −0.48 V (vs. SCE) for **2a**, −0.60 for **2b**, and −0.68 V for [Fe(OEP)(SPh)], respectively. The redox potential is significantly positive-shifted than the reported value (−0.52 V) for singly hydrogen-bonded complex, [Fe^{III}(OEP)(S-2-CF$_3$CONHC$_6$H$_4$)]. The less reversibility ($I_{pa}/I_{pc} = 0.33$ for **2a** 0.49 for **2b**) in the comparison with reported compounds [7] is caused by unstable Fe^{II}–S bond. When the iron(III) is reduced to iron(II), the electron density on the iron center increases, which results in the decrease of electron donation from S to Fe.

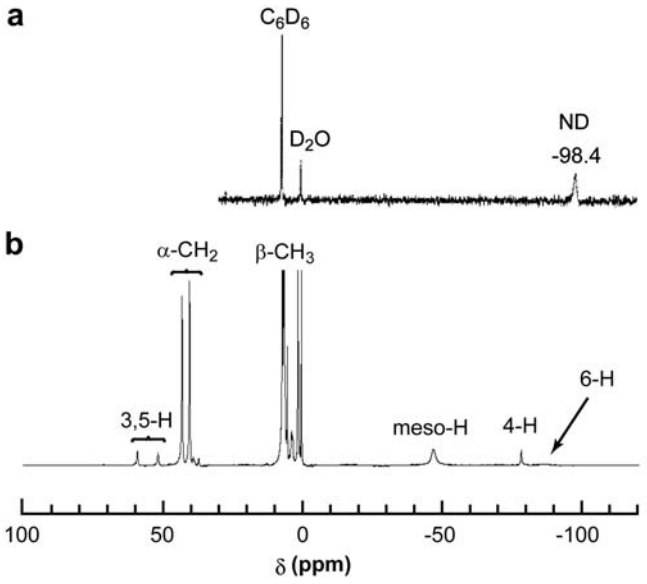

Fig. 3. (a) ^2H NMR spectrum of [Fe^{III}(OEP)(S-2-FcNDCOC$_6$H$_4$)] in benzene and (b) ^1H NMR spectrum of [Fe^{III}(OEP)(S-2-FcNHCOC$_6$H$_4$)] (**2a**) in benzene-d_6 at 30 °C.

Table 5
Electrochemical properties of the compounds in CH_2Cl_2

Compounds	$E_{1/2}$ vs. Ag/Ag^+	
	Fc (Fe^{III}/Fe^{II})[a]	[$Fe^{III/II}$(OEP)(SR)]
2-FcNHCOC$_6$H$_4$SH (**1a**)	98	–
4-FcNHCOC$_6$H$_4$SH (**1b**)	80	–
[Fe^{III}(OEP)(S-2-FcNH-COC$_6$H$_4$)] (**2a**)	72	−770
[Fe^{III}(OEP)(S-4-FcNH-COC$_6$H$_4$)] (**2b**)	57	−890
[Ga^{III}(OEP)(S-2-FcNH-COC$_6$H$_4$)] (**3a**)	65	–
[Ga^{III}(OEP)(S-4-FcNH-COC$_6$H$_4$)] (**3b**)	43	–

[a] Non-substituted ferrocene shows $E_{1/2} = 191$ mV under the same conditions.

Table 4
^1H NMR chemical shifts (ppm) for [Fe^{III}(OEP)(SAr)] (SAr = S-2-FcNHCOC$_6$H$_4$ (**2a**), S-4-FcNHCOC$_6$H$_4$ (**2b**)) in benzene-d_6

Complexes	*meso*-H	α-CH_2	β-CH_3	2,6-H	3,5-H	4-H	NH[a]
2a	−46.7	42.9, 39.9	6.6	−87.0	58.9, 51.6	−78.0	−98.4
2b	−47.6	39.2, 38.0	6.2	−94.4	58.9	–	33.7

[a] ^2H NMR in benzene.

3. Discussion

3.1. Hydrogen bonds in solution and in the solid state

The thiol, **1a**, is intermolecularly NH···O=C hydrogen bonded in the crystal, which is established by X-ray analysis and IR spectra. When it is dissolved in a less polar solvent such as dichloromethane or chloroform, intramolecular SH···O=C hydrogen bond is formed instead of the cleavage of intermolecular hydrogen bonds, which should be preferable in a dilute solution. Such a behavior has been found generally in many compounds with hydrogen bonding ability. In this case, the formation of SH···O=C bond minimizes the total energy in solution. IR and ^{1}H NMR spectra support the presence of this competitive formation of hydrogen bond.

In the thiolate compounds, remarkably strong hydrogen bonds were found in both solution and the solid state. The strongest hydrogen bond was detected in thiolate anion, **4a**, by IR and ^{1}H NMR spectra. The strength of hydrogen bond is estimated by IR and ^{1}H NMR spectra using characteristic NH stretching band and the chemical shift of amide proton. Extraordinary values, 14.21 ppm (chemical shift of NH) and 3044 cm^{-1} (ν(NH)), strongly suggest the presence of exceedingly strong hydrogen bonds. Strong interaction through NH···S hydrogen bond was also found in paramagnetic shift of NH (ca. −100 ppm) for **2a**. Previously, we reported a strong intramolecular NH···S hydrogen bond in five-membered ring of 2-acylaminobenzenethiolate; however the IR and ^{1}H NMR data did not show such a large shift [12]. In six-membered ring described in this paper, the location and direction of amide NH toward the neighboring thiolate are the most appropriate to the formation of hydrogen bonds. Furthermore, the electron-deficient ferrocenyl group efficiently decreases the electron density on NH, which results in the increase of hydrogen bonding ability [16,18]. Replacement of ferrocenyl group by alkyl group, that is (NEt_4)[S-2-*t*-BuNH-COC_6H_4], increases ν(NH) to 3153 cm^{-1} in chloroform [15]. When a metal ion coordinates to the thiolate, the electron density on S decreases by electron donation from sulfur atom to the electron-deficient metal ion. The degree of electron donation depends on the M–S bond character. Ionic Ga–S bond tends to remain the electron on sulfur but the relatively covalent Fe–S bond uses the electrons for the linkage [14]. The found tendency of hydrogen bond strength, **4a** > **2a** > **3a**, is a reasonable result.

3.2. Significant contribution of the hydrogen bonds to M–S bond length

We have systematically demonstrated the contribution of NH···S hydrogen bonds to the M–S bond lengths. In the case of porphyrins, it has been found that the hydrogen bond elongates the M–S bond at the axial position [8,14]. This fact is explained by the decrease of π-donation capability of thiolato ligand by the adjacent amide NH. The geometrical differences from [Ga^{III}(OEP)(SPh)] are listed in Table 1. The significant elongation of Ga–S bond reflects the effectively strong NH···S hydrogen bond of **3a**. The reported structural similarity between Ga^{III} and Fe^{III} porphyrin complexes [14] and spectral data ensure the validity of the analogy despite the structure of **3b** has not been determined.

3.3. Electrochemical contribution of the hydrogen bonds and π-conjugation to the redox potential

The electrochemical interactions through SH···O=C and NH···S hydrogen bonds are illustrated in Fig. 4 with each redox potential vs. Ag/Ag$^+$ in acetonitrile. Inductive effects are evaluated by non-hydrogen-bonded **1b**. When SH···O=C hydrogen bond is formed, the electron on carbonyl oxygen is used to form H···O bond and the deficiency of electron on O is supplied from ferrocene moiety through π-conjugation of amide group. The observed more positive redox potential of **1a** than **1b** is explained reasonably. In contrast to this, the formation of NH···S hydrogen bond results the opposite flow of electrons. When the electron on sulfur is used to form H···S bond, the electron density of sulfur should decrease and the N-Fc moiety becomes electron-rich. The metalloporphyrin supplies electron to the electron-deficient sulfur or the donation from sulfur to metal ion decreases. Consequently, the redox potential of ferrocene should shift negatively. In more ionic Ga–S bond, negative charge on the sulfur atom remains, which results more negative redox potential of ferrocenyl group. The unexpected small values for the 4-substituted derivatives (**2b** and **3b**) are probably caused by efficient substituent effect, that is the *p*-substituent of benzene ring permits electron flow from thiolate anion to the ferrocenyl

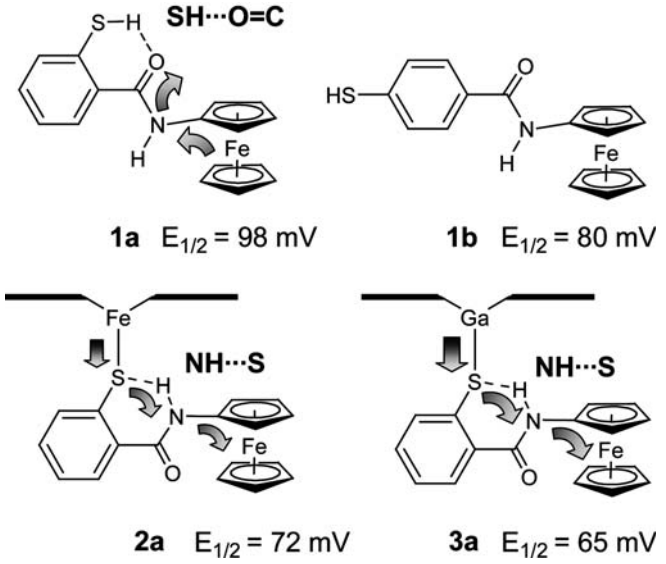

Fig. 4. Electronic interaction through intermolecular NH···S and SH···O=C hydrogen bonds in **1a, 2a**, and **3a**. The arrows indicate schematically the electron flow. The redox potentials ($E_{1/2}$) are shown vs. Ag/Ag$^+$ in acetonitrile.

group through π-conjugation system in quionid form. In the case of **2a** and **3a**, part of the electrons is used for the hydrogen bond and the localization of electron there presumably restricts the effective flow of electron to the ferrocene moiety, which results a small positive shift.

4. Conclusions

The redox-active thiolate ligand having ferrocene moiety provided a delicate detection of the electron flow through SH···O=C and NH···O=C hydrogen bonds. In the porphyrin-thiolate compounds, the electron flows from porphyrin to ferrocene through NH···S hydrogen bond and π-conjugation system were detected. The electron-deficient ferrocene moiety strengthens NH···S hydrogen bond resulting a significantly long M–S bond and a remarkably positive redox potential of metalloporphyrin.

5. Experimental

All procedures were performed in argon atmosphere by Schlenk technique. All solvents except for water were dried over calcium hydride and distilled under argon before use. The synthetic procedures of acetylaminoferrocene [17], aminoferrocene [16], and [Ga^{III}(OEP)(OMe)] (OEP = octaethylporphinato) [14] were described in the previous paper. [Fe^{III}(OEP)(OMe)] was synthesized by the literature method [20].

5.1. 2,2′-Dithiobis(N-ferrocenylbenzamide)

A mixture of 2,2′-dithiodibenzoic acid (2.97 g, 9.71 mmol), thionyl chloride (20 mL) and a catalytic amount of DMF (two drops) was refluxed for 3 h. And then excess thionyl chloride was removed in vacuo, and the residue was dissolved in THF (50 mL). The solution was added slowly to a solution of aminoferrocene (3.90 g, 19.4 mmol) and triethylamine (2.69 mL, 19.4 mmol) in THF (10 mL) at 0 °C. After stirring overnight at room temperature, the solution was concentrated to dryness under reduced pressure. The residue was suspended in ethyl acetate (300 mL) and insoluble product was collected with filtration. The product was washed with $NaHCO_3$ aq and water, and then dried in vacuo. Yield: 4.20 g (47%). ^{1}H NMR (303 K, dimethyl sulfoxide-d_6): δ 4.02 (s, 4H, Cp), 4.17 (s, 10H, Cp), 4.76 (s, 4H, Cp), 7.34 (t, 2H, $J = 8.0$ Hz, Ph), 7.48 (t, 2H, $J = 8.0$ Hz, Ph), 7.63 (d, 2H, $J = 8.0$ Hz, Ph), 7.72 (d, 2H, $J = 8.0$ Hz, Ph), 9.99 (s, 2H, NH). Anal. Calc. for $C_{34}H_{28}Fe_2N_2O_2S_2 \cdot (H_2O)_{0.8}$: C, 59.46; H, 4.34; N, 4.08. Found: C, 59.47; H, 4.10; N, 4.09. MS (ESI): Calc. $m/z = 672.0$ (M^+); Found 672.0.

5.2. 2-Mercapto-N-ferrocenylbenzamide, 2-FcNHCOC$_6$H$_4$SH (**1a**)

To the suspension of 2,2′-dithiobis(*N*-ferrocenylbenzamide) (50 mg, 0.074 mmol) in ethanol (3 mL) was added $NaBH_4$ (90 mg, 2.3 mmol) and stirred overnight. The resulting clear solution was concentrated under reduced pressure, and then 2 M HCl aq was added. The product was extracted with ethyl acetate and the organic layer was washed with saturated NaCl aqueous solution and dried over anhydrous sodium sulfate. Removal of solvents gave the product. Yield: 36 mg (73%). ^{1}H NMR (303 K, chloroform-d_1): δ 4.06 (s, 2H, Cp), 4.22 (s, 5H, Cp), 4.66 (s, 1H, SH), 4.71 (s, 2H, Cp), 7.10 (br, 1H, NH), 7.20 (t, 1H, $J = 6.0$ Hz, Ph), 7.30 (t, 1H, $J = 6.0$ Hz, Ph), 7.37 (d, 1H, $J = 7.6$ Hz, Ph), 7.48 (d, 1H, $J = 7.6$ Hz, Ph). Anal. Calc. for $C_{17}H_{15}Fe_1N_1O_1S_1 \cdot (H_2O)_{0.8}$: C, 59.91; H, 4.55; N, 4.11. Found: C, 59.73; H, 4.45; N, 4.18. MS (ESI): Calc. $m/z = 338.0$ ($M+H^+$); Found 338.0.

5.3. Tetramethylammonium 2-(ferronyl carbamoyl)benzenethiolate, (NEt$_4$)[S-2-FcNHCOC$_6$H$_4$] (**4a**)

Tetramethylammonium thiophenolate (181 mg, 0.46 mmol) and 2,2′-dithio bis(*N*-ferrocenyl benzamide) (200 mg, 0.30 mmol) were dissolved in EtOH (8 mL). After stirred for 1 h, the precipitate was removed by filtration. The solvent was removed under reduced pressure. The crude product was recrystallized from CH_3CN/diethyl ether. ^{1}H NMR ($CDCl_3$): δ 1.12 (12H, t, $J = 6.8$ Hz, CH_3), 3.04 (8H, q, $J = 7.2$ Hz, CH_2), 3.98 (2H, s, Cp), 4.19 (5H, s, Cp), 4.79 (2H, s, Cp), 6.77 (1H, t, $J = 7.6$ Hz, Ph), 6.90 (1H, t, $J = 7.6$ Hz, Ph), 7.64 (1H, d, $J = 8.0$ Hz, Ph), 8.16 (1H, d, $J = 8.0$ Hz, Ph), 14.23 (1H, br, NH).

5.4. 4,4′-Dithiodibenzoic acid

Crystallized sodium sulfide ($Na_2S \cdot 9H_2O$, 19.0 g, 79.2 mmol) and powdered sulfur (2.54 g, 79.4 mmol) were dissolved in water (20 mL) by heating and stirring. An aqueous solution (8 mL) of NaOH (3.0 g, 75 mmol) was added to the solution, and cooled to 0 °C. *para*-Aminobenzoic acid (10.0 g, 72.9 mmol) was dissolved in a mixture of water (80 mL) and concentrated hydrochloric acid (15 mL), and cooled to 0 °C. An aqueous solution of $NaNO_2$ (5.02 g, 72.8 mmol) was added to the solution of Na_2S and sulfur below 5 °C. And this solution was added to the solution of *p*-aminobenzoic acid below 5 °C. The mixture was stirred for 1 h at 0 °C, and continued stirring for 2 h at room temperature. Addition of 6 M HCl aq (20 mL) gave precipitate, which was collected with filtration, and washed with water, *n*-hexane and diethyl ether. The precipitate was dissolved in 1MNaOH aq (30 mL), and removed the precipitate with filtration. Addition of concentrated hydrochloric acid (25 mL) to the filtrate gave precipitate, which was collected with filtration, and washed with water and diethyl ether. The residue was recrystallized from THF/diethyl ether. Yield: 1.67 g (15%) ^{1}H NMR (dimethyl sulfoxide-d_6): δ 7.64 (4H, d, $J = 8.4$ Hz, Ph), 7.93 (4H, d, $J = 8.4$ Hz, Ph), 9.99 (2H, br, COOH). MS (ESI): Calc. $m/z = 305.0$ ($M-H^+$); Found 305.0.

5.5. 4,4′-Dithiobis(N-ferrocenylbenzamide)

A suspension of 4,4′-dithiodibenzoic acid (502 mg, 1.64 mmol), thionyl chloride (4 mL) and a catalytic amount of DMF (two drops) was refluxed for 1 h. And then excess thionyl chloride was removed in vacuo, and the residue was dissolved in THF (20 mL). The solution was added slowly to a THF solution (5 mL) of aminoferrocene (722 mg, 3.59 mmol) and triethylamine (0.5 mL, 3.59 mmol) at 0 °C. The solution was stirred overnight at room temperature. Then the solution was concentrated to dryness under reduced pressure, and the residue was washed with ethyl acetate (300 mL) and water (200 mL) to remove soluble materials. The insoluble product was collected with filtration, washed with 4% $NaHCO_3$ aq and water, and then dried in vacuo over P_2O_5. Yield: 725 mg (66%). ^{1}H NMR (303 K, dimethyl sulfoxide-d_6): δ 4.03 (s, 4H, Cp), 4.11 (s, 10H, Cp), 4.77 (s, 4H, Cp), 7.67 (d, 4H, $J = 8.4$ Hz, Ph), 7.92 (d, 4H, $J = 8.0$ Hz, Ph), 9.73 (br, 2H, NH). Anal. Calc. for $C_{34}H_{28}Fe_2N_2O_2S_2 \cdot (H_2O)_{0.8}$: C, 59.46; H, 4.34; N, 4.08. Found: C, 59.51; H, 4.36; N, 4.15. MS (ESI): Calc. $m/z = 672.0$ (M^+); Found 672.0.

5.6. 4-Mercapto-N-ferrocenylbenzamide, 4-FcNHCOC$_6$H$_4$SH (**1b**)

To the suspension of 4,4′-dithiobis(*N*-ferrocenylbenzamide) (200 mg, 0.29 mmol) in a mixture of ethanol (8 mL) and THF (18 mL) was added $NaBH_4$ (350 mg, 9.3 mmol) and the mixture was stirred overnight. The resulting clear solution was concentrated under reduced pressure, and then 2 M HCl aq was added to the residue. The precipitate was extracted with ethyl acetate. The organic layer was washed with saturated NaCl aq and dried over anhydrous sodium sulfate. The solution was concentrated to dryness under reduced pressure and then dried over P_2O_5. Yield: 132 mg (68%). ^{1}H NMR (303 K, chloroform-d_1): δ 3.59 (1H, s, SH), 4.06 (s, 2H, Cp), 4.19 (s, 5H, Cp), 4.71 (s, 2H, Cp), 7.09 (br, 1H, NH), 7.33 (d, 2H, $J = 8.0$ Hz, Ph), 7.67 (d, 1H, $J = 8.0$ Hz, Ph). Anal. Calc. for $C_{174}H_{15}FeNOS \cdot (H_2O)_{0.7}$: C, 58.37; H, 4.73; N, 4.00. Found: C, 58.34; H, 4.61; N, 4.06. MS (ESI): Calc. $m/z = 337.0$ (M^+); Found 337.0.

5.7. Tetraethylammonium 4-(N-ferronycarbamoyl) benzenethiolate, (NEt$_4$)[S-4-FcNHCOC$_6$H$_4$] (**4b**)

Tetraethylammonium thiophenolate (92.2 mg, 0.385 mmol) and 4-mercapto-*N*-ferrocenylbenzamide (125 mg, 0.372 mmol) were dissolved in EtOH (10 mL). After stirred for 5 h, the precipitate was removed with filtration. The solvent was removed under reduced pressure. The crude product was recrystallized from CH_3CN and diethyl ether. ^{1}H NMR ($CDCl_3$): δ 1.19 (12H, t, $J = 6.8$ Hz, CH_3), 3.16 (8H, q, $J = 7.2$ Hz, CH_2), 3.98 (2H, s, Cp), 4.16 (5H, s, Cp), 4.91 (2H, s, Cp), 7.45 (2H, d, $J = 8.0$ Hz, Ph), 7.50 (2H, d, $J = 8.4$ Hz, Ph), 8.26 (1H, s, NH).

5.8. [Fe^{III}(OEP)(S-2-FcNHCOC$_6$H$_4$)] (**2a**)

[Fe^{III}(OEP)(OMe)] (19.86 mg, 32.0 μmol) and **1a** (10.68 mg, 31.7 μmol) were dissolved in 30 mL of toluene. The mixture was stirred for 1 h at room temperature. Removal of the solvent gave purple solid in a quantitative yield. ^{1}H NMR (303 K, benzene-d_6): δ −98.4 (1H, NH), −87.0 (1H, Ph 6-H), −78.0 (1H, Ph 4-H), −46.7 (4H, *meso*-H), 1.48 (2H, Cp), 1.57 (5H, Cp), 5.40 (2H, Cp), 6.6 (24H, β-CH_3), 42.9, 42.9, 39.9 (16H, α-CH_2), 58.9, 51.6 (2H, Ph 3,5-H). MS (ESI): Calc. $m/z = 924.3$ (M^+); Found 924.3.

5.9. [Fe^{III}(OEP)(S-4-FcNHCOC$_6$H$_4$)] (**2b**)

[Fe^{III}(OEP)(OMe)] (20.23 mg, 32.6 μmol) and **1b** (10.94 mg, 32.4 μmol) were dissolved in 30 mL of toluene. The mixture was stirred for 1 h at room temperature. Removal of the solvent gave purple solid in a quantitative yield. ^{1}H NMR (303 K, benzene-d_6): δ −94.4 (1H, Ph 2,6-H), −47.6 (4H, *meso*-H), 3.88 (2H, Cp), 4.02 (5H, Cp), 4.51 (2H, Cp), 6.18 (24H, β-CH_3), 33.7 (1H, NH), 38.0, 39.2 (16H, α-CH_2), 58.9 (2H, br, Ph 3,5-H). MS (ESI): Calc. $m/z = 924.3$ (M^+); Found 923.9.

5.10. [Ga^{III}(OEP)(S-2-FcNHCOC$_6$H$_4$)] (**3a**)

[Ga^{III}(OEP)(OMe)] (40 mg, 63.1 μmol) and **1a** (21.3 mg, 63.1 μmol) were dissolved in 8 mL of dichloromethane. The mixture was stirred for 1 h at room temperature. The solvent was removed under reduced pressure to give a crude product, which was recrystallized from toluene/acetonitrile. Yield: 15 mg (25%). ^{1}H NMR (303 K, benzene-d_6): δ 1.87 (t, 24H, $J = 7.6$ Hz, β-CH_3), 3.53 (s, 5H, Cp), 3.57 (d, 1H, $J = 7.6$ Hz, Ph 6-H), 4.04 (s, 2H, Cp), 3.91, 4.02 (m, 16H, α-CH_2), 4.29 (s, 2H, Cp), 6.03 (t, 1H, $J = 7.6$ Hz, Ph 4-H), 6.59 (t, 1H, $J = 7.6$ Hz, Ph 5-H), 7.75 (s, 1H, NH), 8.01 (d, 1H, $J = 8.0$ Hz, Ph 3-H), 10.22 (s, 4H, *meso*-H). MS (ESI): Calc. $m/z = 938.3$ ($M+H^+$); Found 938.1.

5.11. [Ga^{III}(OEP)(S-4-FcNHCOC$_6$H$_4$)] (**3b**)

[Ga^{III}(OEP)(OMe)] (107 mg, 169 μmol) and **1b** (57.5 mg, 170 μmol) were dissolved in 45 mL of toluene. The mixture was stirred for 1 h at room temperature. The solvent was removed under reduced pressure to give a crude product, which was recrystallized from THF/toluene. Yield: 67 mg (42%). ^{1}H NMR (303 K, chloroform-d_1): δ 1.96 (t, 24H, $J = 7.6$ Hz, β-CH_3), 3.74 (s, 5H, Cp), 3.83 (d, 2H, $J = 7.6$ Hz, 2, 6-H), 4.17 (m, 20H, α-CH_2, Cp), 6.52 (s, 1H, NH), 6.90 (d, 2H, $J = 7.6$ Hz, Ph 3,5-H), 10.31 (s, 4H, *meso*-H). MS (ESI): Calc. $m/z = 938.3$ ($M+H^+$); Found 938.1.

5.12. Physical measurements

The ^{1}H NMR spectra were measured on a Jeol GSX-400 spectrometer. IR spectra were recorded on a Jasco FT/IR-8300 spectrometer. Samples were prepared as CH_2Cl_2 solution or KBr pellet. Electrochemical measurements were carried out on a BAS 100 B/W using three electrode method. Sample was prepared as 2.5 mM CH_2Cl_2 solution including 0.2 M tetra-*n*-butylammonium perchlorate as a supporting electrolyte. Scan rate was 100 mV/s. $E_{1/2}$ value was referenced to non-aqueous Ag/Ag^+ electrode at room temperature. ESI-MS spectra were measured on a Finnigan mat LCQ ion trap spectrometer using methanol solution.

5.13. X-ray crystallography

5.13.1. 2-FcNHCOC$_6$H$_4$SH (**1a**)

A suitable single orange crystal grown from ethyl acetate was shielded in a glass capillary under argon atmosphere. X-ray measurement was performed at 23 °C using the ω scan technique up to $2\theta_{max} = 55°$ on a Rigaku AFC5R diffractometer with graphite monochromated MoKα radiation (0.71069 Å). Unit cell dimensions were obtained by least-square refinement with 25 reflections. Three standard reflections were chosen and their intensities did not change during the data collection. The structure was solved by direct method (SIR92) [21] using teXsan crystallographic software package of the Molecular Structure Corporation. Refinements were carried out on F^2. All non-hydrogen atoms were refined anisotropically. The carbon-bonded hydrogen atoms were placed in the calculated positions. The nitrogen and sulfur-bonded hydrogen atoms were located from a difference Fourier map. The position of the hydrogen atom of thiol group is refined using the fixed isotropic thermal factor.

5.13.2. Crystallographic data for **1a**

$C_{17}H_{15}ONSFe$, fw 337.22, orthorhombic, space group *Pbca*, $a = 25.308(3)$, $b = 11.157(2)$, $c = 10.357(3)$ Å, $V = 2924(1)$ Å^3, $Z = 8$, $F(000) = 1392$, $d_{calc} = 1.532$ g cm^{-3}, $\mu = 1.169$ mm^{-1}, 3365 unique reflections, $R_1 = 0.0345$ [$I > 2.0\sigma(I)$], $wR_2 = 0.103$ (all data), GOF 1.00, 193 parameters.

5.13.3. [Ga^{III}(OEP)(S-2-FcNHCOC$_6$H$_4$)] (**3a**)

A single crystal of was mounted in a fine nylon loop with Nujol and immediately freezed at −50 °C. All measurements were made on a Rigaku RAXIS-RAPID Imaging Plate diffractometer with graphite monochromated MoKα radiation. The structure was solved by direct method (SIR92) [21] and the following refinements were performed using SHELXL-97 [22] and teXsan crystallographic software package. All non-hydrogen atoms were refined anisotropically and hydrogen atoms were placed in the calculated positions and including least-square refinement.

5.13.4. Crystallographic data for **3a**

$C_{58.5}H_{65}ON6SGaFe$, fw 1025.8, triclinic, space group $P\bar{1}$, $a = 15.02(2)$, $b = 17.12(2)$, $c = 21.12(2)$ Å, $\alpha = 109.32(4)°$, $\beta = 97.04(4)°$, $\gamma = 91.51(5)°$, $V = 5075(11)$ Å^3, $Z = 4$, $F(000) = 2156$, $d_{calc} = 1.343$ g cm^{-3}, $\mu = 0.905$ mm^{-1}, 17597 unique reflections, $R_1 = 0.0573$ [$I > 2.0\sigma(I)$], $wR_2 = 0.0742$ (all data), GOF 1.00, 1190 parameters.

Acknowledgement

This work was supported by the Grant-in-Aid from the Ministry of Education, Culture, Sports, Science, and Technology.

Appendix A. Supplementary material

Crystallographic data for structural analysis have been deposited with the Cambridge Crystallographic Data Centre, CCDC Nos. 299299 and 299300 for compounds **1a** and **3a**. Copies of this information may be obtained free of charge from The Director, Cambridge Crystallographic Data Centre, 12 Union Road, Cambridge CB2 1EZ, UK (fax: +44 1223 336003; e-mail: deposit@ccdc.cam.ac.uk or www: http://www.ccdc.cam.ac.uk). Supplementary data associated with this article can be found, in the online version, at doi:10.1016/j.jorganchem.2006.08.067.

References

[1] P.D. Beer, P.A. Gale, Angew. Chem., Int. Ed. 40 (2001) 486.
[2] P.D. Beer, J.J. Davis, D.A. Drillsma-Milgrom, F. Szemes, Chem. Commun. (2002) 1716.
[3] X. Cui, R. Delgado, H.M. Carapuça, M.G.B. Drew, V. Félix, Dalton Trans. (2005) 3297.
[4] S.R. Collinson, T. Gelbrich, M.B. Hursthouse, J.H.R. Tucker, Chem. Commun. (2001) 555.
[5] J. Westwood, S.J. Coles, S.R. Collinson, G. Gasser, S.J. Green, M.B. Hursthouse, N.E. Light, J.H.R. Tucker, Organometallics 23 (2004) 946.
[6] K. Kavallieratos, S. Hwang, R.H. Crabtree, Inorg. Chem. 38 (1999) 5184.
[7] N. Ueyama, N. Nishikawa, Y. Yamada, T. Okamura, S. Oka, H. Sakurai, A. Nakamura, Inorg. Chem. 37 (1998) 2415.
[8] T. Okamura, S. Takamizawa, N. Ueyama, A. Nakamura, Inorg. Chem. 37 (1998) 18.
[9] N. Ueyama, Y. Yamada, T. Okamura, S. Kimura, A. Nakamura, Inorg. Chem. 35 (1996) 6473.
[10] N. Ueyama, N. Nishikawa, Y. Yamada, T. Okamura, A. Nakamura, J. Am. Chem. Soc. 118 (1996) 12826.
[11] N. Ueyama, T. Okamura, A. Nakamura, J. Chem. Soc., Chem. Commun. (1992) 1019.
[12] T. Okamura, N. Ueyama, A. Nakamura, E.W. Ainscough, A.M. Brodie, J.M. Waters, J. Chem. Soc., Chem. Commun. (1993) 1658.
[13] N. Ueyama, T. Okamura, A. Nakamura, J. Am. Chem. Soc. 114 (1992) 8129.
[14] T. Okamura, N. Nishikawa, N. Ueyama, A. Nakamura, Chem. Lett. (1998) 199.
[15] M. Kato, K. Kojima, T. Okamura, H. Yamamoto, T. Yamamura, N. Ueyama, Inorg. Chem. 44 (2005) 4037.
[16] T. Okamura, K. Sakauye, M. Doi, H. Yamamoto, N. Ueyama, Bull. Chem. Soc. Jpn. 78 (2005) 1270.
[17] T. Okamura, K. Sakauye, N. Ueyama, A. Nakamura, Inorg. Chem. 37 (1998) 6731.

[18] T. Okamura, N. Ueyama, Metal–Hydrogen Bond Conjugated Systems, in: A. Nakamura, N. Ueyama, K. Yamaguchi (Eds.), Organometallic Conjugation, Kodansha, Tokyo, 2002, pp. 307–330.
[19] S.C. Tang, S. Koch, G.C. Papaefthymiou, S. Foner, R.B. Frankel, J.A. Ibers, R.H. Holm, J. Am. Chem. Soc. 98 (1976) 2414.
[20] K. Hatano, T. Uno, Chem. Soc. Jpn. 63 (1990) 1825.
[21] A. Altomare, M.C. Burla, M. Camalli, M. Cascarano, C. Giacovazzo, A. Guagliardi, G. Polidori, J. Appl. Crystallogr. 27 (1994) 435.
[22] G.M. Scheldrick, SHELXL-97, Program for Crystal Structure Solution and Refinement, University of Gottingen, Germany, 1997.